

See discussions, stats, and author profiles for this publication at: <https://www.researchgate.net/publication/231232128>

Growth Behavior, Microstructure Characterization, and Field-Emission Property of 6-Fold Hierarchical Zn/ZnO Structures Prepared by Direct Annealing

ARTICLE in CRYSTAL GROWTH & DESIGN · JANUARY 2009

Impact Factor: 4.89 · DOI: 10.1021/cg800373u

CITATIONS

14

READS

16

4 AUTHORS, INCLUDING:



Ing-Chi Leu

National University of Tainan

124 PUBLICATIONS 1,880 CITATIONS

SEE PROFILE

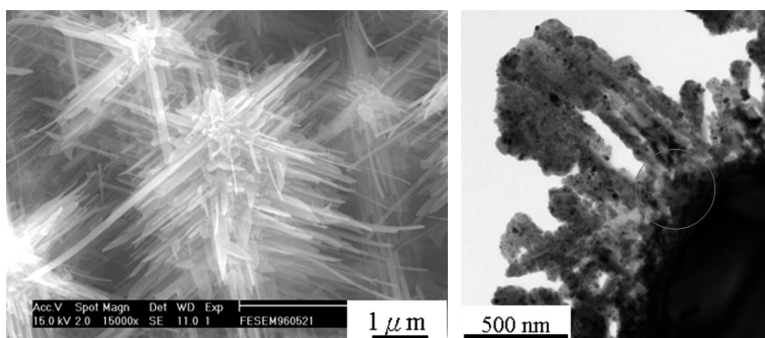
Article

Growth Behavior, Microstructure Characterization, and Field-Emission Property of 6-Fold Hierarchical Zn/ZnO Structures Prepared by Direct Annealing

Chi-Yun Kuan, Min-Hsiung Hon, Jaw-Min Chou, and Ing-Chi Leu

Cryst. Growth Des., **2009**, 9 (2), 813-819 • DOI: 10.1021/cg800373u • Publication Date (Web): 20 January 2009

Downloaded from <http://pubs.acs.org> on February 13, 2009



More About This Article

Additional resources and features associated with this article are available within the HTML version:

- Supporting Information
- Access to high resolution figures
- Links to articles and content related to this article
- Copyright permission to reproduce figures and/or text from this article

[View the Full Text HTML](#)



ACS Publications
High quality. High impact.

Growth Behavior, Microstructure Characterization, and Field-Emission Property of 6-Fold Hierarchical Zn/ZnO Structures Prepared by Direct Annealing

Chi-Yun Kuan,[†] Min-Hsiung Hon,[†] Jaw-Min Chou,[‡] and Ing-Chi Leu^{*,§}

Department of Materials Science and Engineering, National Cheng Kung University, Tainan 701, Taiwan, ROC, Department of Materials Science and Engineering, I-Shou University, Kaohsiung Hsien 840, Taiwan, ROC, and Department of Material Science, National University of Tainan, Tainan 700, Taiwan, ROC

Received April 10, 2008; Revised Manuscript Received November 16, 2008

ABSTRACT: Six-fold core-shelled three-dimensional hierarchical structures were prepared by a direct annealing process. The effect of experimental parameters on density and length of branches of hierarchical Zn/ZnO structure is discussed. The influence of oxide layer formation and the shape of Zn polyhedron on the relaxation of stress for nanostructure growth also is reported. At the annealing temperature of 375 °C, the largest aspect ratio (~71) of branched nanostructures and the smallest density (0.05 tips/ μm^2) of hierarchical arrays can be obtained. Transmission electron microscopy analysis shows that the oxide layer grows epitaxially from the Zn microtips and then the branches grow epitaxially from the oxide layer. For field emission applications, a better turn-on electric field (8.5 V/ μm) and a larger enhancement factor 3490 are obtained for branched nanostructures with the high aspect ratio.

Introduction

Semiconductor materials have attracted a great deal of attention owing to their interesting optical, electric, and catalytic properties. Recently, nanostructures of various semiconductor materials, such as TiO_2 , WO_3 , and ZnO, have been synthesized due to the realization of their applications in different fields. Nanostructured ZnO materials have emerged as one of the most promising oxide materials due to their distinguished performance in electronics, optics, and photonics. Besides, ZnO is a versatile functional material that has a diverse group of growth morphologies, such as nanorings, nanohelices/nanosprings, nanobelts,¹ nanowires, and nanorods.² For the synthesis of ZnO nanostructures, many different approaches have been developed, such as thermal evaporation,¹ solution-phase deposition,² and electrophoretic deposition with template.³ ZnO single crystals exhibit a wide range of novel structures that can be grown by tuning the growth rates along different crystal directions.⁴ One of the most profound factors determining the morphology involves the relative surface activities of various growth facets under given conditions. Macroscopically, the crystal growth has different kinetic parameters for different crystal planes, which can be emphasized under controlled growth conditions.

The novel well-defined three-dimensional (3D) ZnO nanostructure is of significant importance for fundamental research as well as for various relevant applications. For hierarchical structures, several preparation strategies exist, such as vapor–liquid–solid process⁵ and solution-phase process,⁶ to meet the current requirements and future challenges. However, the simplicity and low cost for both process and equipment make the method especially competitive for the fabrication of one-dimensional nanostructure arrays.⁷ An alternative strategy is to grow nanostructure arrays directly from metal substrates so that the nanostructure synthesis and assembly are accomplished in one step without templates. The requirement for low synthesis

temperature is more feasible by using the direct oxidation of metallic foil for fabricating semiconductor nanostructures^{7,8} than those using the conventional thermal evaporation process.^{1,5} So far, several studies regarding the direct oxidation of zinc or zinc-alloy metallic by annealing treatment have been reported.^{8–10} Using direct annealing of either zinc or zinc alloy, one-dimensional nanostructures are formed on the surface. By further controlling the annealing temperature and composition of metallic foil, the morphologies obtained are different. However, the anisotropic, symmetric, and well-defined 3D hierarchical structure cannot be obtained under these experimental conditions. In the present study, the hierarchical structure is obtained by direct thermal oxidation of metallic foil with single crystalline Zn microtips arrays, and 6-fold core-shelled 3D hierarchical structures are observed. The method has the virtue of simplicity, efficiency, and low cost, which facilitates device fabrication and characterizations. There are two main processes about the hierarchical structures formation: formation of oxide layer and growth of branched nanostructures. However, the relationship among characteristics of microtips arrays, oxide layer formation, and branched nanostructures growth have not been identified elsewhere. The influence of experimental parameters, such as temperature, time, and growth atmosphere, on the 3D hierarchical structure formation procedure has not been explained. Therefore, in the present study, a systematical investigation on the branch formation mechanism has been explored. The primary goal of this research is to develop a fundamental model of stress evolution on single-crystalline Zn microtips and its effect on the growth of branch structures.

Experimental Procedures

Two types of substrates were provided for annealing treatment, such as polycrystalline Zn foil and single-crystalline Zn microtips arrays. A polycrystalline Zn foil (99.9%, Alfa Aesar) was mechanically polished, and followed by electropolishing with a 2:1 mixture of 99.8% ethanol and 85% phosphoric acid at a current density of 69 mA cm^{-2} for 10 min. The single-crystalline Zn pyramid microstructures were prepared by anodic etching on polycrystalline Zn foil, which was conducted in solution of $\text{NH}_4\text{Cl}/\text{H}_2\text{O}_2$ with a molar ratio of 32 using a constant current density of 55 mA cm^{-2} for 60 s.¹¹ The single-crystalline Zn pyramids were heated at different temperatures (250, 300, 325, 350, 375 °C)

* To whom correspondence should be addressed. Fax: 886-6-2380208. E-mail: icleu@mail.mse.ncku.edu.tw.

[†] National Cheng Kung University.

[‡] I-Shou University.

[§] National University of Tainan.

and times (6, 8, 10, 12 h) in air with a heating rate of 5 °C/min. The hierarchical structures were characterized by a field emission scanning electron microscope (FE-SEM, XL-40FEG, Philips), and the structural properties were studied by transmission electron microscopy (FEG-TEM, Tecnai F20 G2 MAT, FEI). The field emission characteristics were determined in a chamber with a base vacuum of 5×10^{-6} torr, and a Keithley 237 was employed as a power supply and a current meter.

Results and Discussion

Annealing treatment was kept under different temperatures for 12 h in air, and 3D hierarchical structures were obtained above 310 °C, as shown in Figure 1. The original Zn pyramid arrays before annealing treatment and the related TEM microscopic image is shown in Figure 1a. From the SEM and TEM results, the 6-fold polyhedrons of single-crystalline Zn can be obtained. When the annealing is kept at 250 °C for 12 h, the single crystalline metallic Zn pyramids are essentially coated by small particles. Raising the temperature to 300 °C, a few short whiskers are formed in the Zn pyramids surfaces as shown in Figure 1a. As the temperature is increased beyond 310 °C, the branched and 6-fold ZnO nanowhiskers are formed on Zn pyramids as shown in Figure 1b. The 6-fold anisotropic morphology is not observed by further increasing the annealing temperature to 400 °C. Comparing the morphologies of branching ZnO nanowhiskers formed on Zn microtips under different annealing temperature treatments, different lengths of ZnO are obtained. However, the density of microtips for 3D hierarchical structure arrays growth is a function of temperature, as shown in Figure 1d. Increasing annealing temperature from 250 to 375 °C, the density of the 3D hierarchical microtip arrays decreases from 0.49 to 0.05 tips/ μm^2 . The height and intertip spacing of Zn microtip arrays obtained from anodization processes are not uniform,¹¹ and the distance between Zn microtips is about 1–2 μm . However, the longest branched nanowires is 2.5 μm obtained by direct annealing at 375 °C for 12 h, which is larger than the distance between microtips. When the annealing temperature is at 250 °C, a thin oxide layer is formed on the microtip surface and the density of hierarchical microtip arrays is higher. The density of the 3D hierarchical arrays decreases with increasing annealing temperature. In summary, the much longer ZnO branches in 3D hierarchical structure will shadow the lower ones which results in the lowest density (0.05 tips/ μm^2) of the 3D hierarchical arrays at 375 °C.

How the annealing time affects the branching length of ZnO nanowires is investigated by annealing Zn foil at 350 °C for different annealing times as shown in Figure 2a,b. The 6-fold symmetric hierarchical ZnO structure is maintained for different annealing times at 350 °C. The length of branching ZnO nanowires increases from about 0.3 to 1.8 μm by extending the annealing time from 4 to 12 h. It is also evident from Figure 2a,b that the density of hierarchical nanostructure is independent of the annealing time. From the results of annealing treatment, it is clear that the length of the nanowhiskers and the density of hierarchical structures are a function of the annealing time and temperature, respectively. The relationship between annealing time and length of branched ZnO nanowhiskers at different annealing temperatures is illustrated in Figure 2c. For different annealing temperatures, the relationship between length of branched nanowhiskers and annealing time is linearly proportional. From this linear relation, a slope represents the growth rate is thus obtained. The growth rate increases from 0.02 to 0.20 $\mu\text{m}/\text{h}$ with increasing annealing temperature from 310 to 375 °C, and the linear function illustrated in Figure 2d with $y = -12399.6x + 17.9$, can be obtained by plotting

$\ln(\text{growth rate})$ of branched nanostructures (μm) against the reciprocal of annealing temperature ($1/T$ (K)). The linear relationship fitted to the data yields an apparent activation energy of 103.1 kJ/mol. The activation energy for growing Zn-ZnO core-shelled structure (170–372 kJ/mol)¹² has been determined by the self-diffusion of Zn ion at low-temperature. However, under a vapor-phase system, the activation energy for nanostructure branched growth has not yet been explored. The lower activation energy results of the ZnO branches growth obtained by direct annealing may be due to stress relaxation. The theoretical lowest temperature for the nucleation at about 300 °C can be immediately deduced at the x -intercept ($y = 0$, growth rate = 0) of the line (growth rate vs temperatures),¹³ as the inset of Figure 1a. When the annealing temperature is below 300 °C, no ZnO branched nanostructures are found on the Zn 6-fold polyhedron facets even by annealing for 12 h. By increasing the annealing temperature to 300 °C, the nucleation of branches is observed. However, when the length of the branches is increased by increasing the annealing temperature, the shadowing phenomenon is observed. Therefore, the density of hierarchical microtip arrays changes at a distinct temperature of 300 °C owing to the shadowing phenomenon.

Most metals are unstable in air at room temperature, owing particularly to their affinity for oxygen. There is no doubt that the reaction will begin at the metal–gas interface, and will form an intermediate layer between the metal and the gas. Hence, in order to determine the influence of oxygen on forming metal oxide, the result of annealing in a vacuum (10^{-6} torr) is shown in Figure 3 for the sample kept at 350 °C for 2 h. From the results of SEM analysis, the importance of oxygen on the formation of oxide films and branches can be verified. Whether polycrystalline Zn foil or single-crystalline Zn microtips arrays, nanostructures are not obtained under a vacuum. By thermal oxidation of metallic foil, the oxide film will be formed on the surface at first. The formation of oxide layer on zinc can be divided into the steps described as follows:¹⁴ (1) activated absorption of O_2 , (2) conversion of adsorbed O atom into O^- ion by catching electrons that pass from the underlying metal to the oxide–oxygen interface, (3) a vacant V_{Zn} site is formed when a Zn^{2+} ion moves to an adsorbed O^- ion, and (4) Zn^{2+} ions migrate from the metal, through the oxide, to fill these vacancies, thereby forming a layer of ZnO. The growth of oxides on the Zn foil obeys the parabolic equation.^{14,15} The oxidation rate increases with increasing temperature and oxygen partial pressure. In general, during the formation of oxide on the metal–gas interface, the severe biaxial stresses are developed due to the volume expansion of existing oxide layer.¹⁵ The thermal annealing temperature not only affects the oxidation rate but also influences the interfacial stress, surface and interface energies, and elastic properties of the oxide film. At low temperatures, the oxidation rate is low; therefore, the growth of the oxide layer and the accumulation of stress are slow. As long as the oxidation process continues the oxide layer stress is accumulated until a critical limit is reached; the oxide layer relaxes itself by a spontaneous growth of nanostructures from the oxide surface.¹⁶ In other words, the growth of branches is related to the influence of atmosphere on the oxidation processes and the thickness of oxide layer. The growth mechanism for the ZnO branches under low temperatures is not only related to thermal oxidation of Zn microtips but also the mass transfer path of vapors, such as paths for oxygen and zinc. Although the operating temperature is low (250–375 °C) in the present study, the possibility of the involvement of Zn vapor mass transfer cannot be completely excluded in the reaction due to

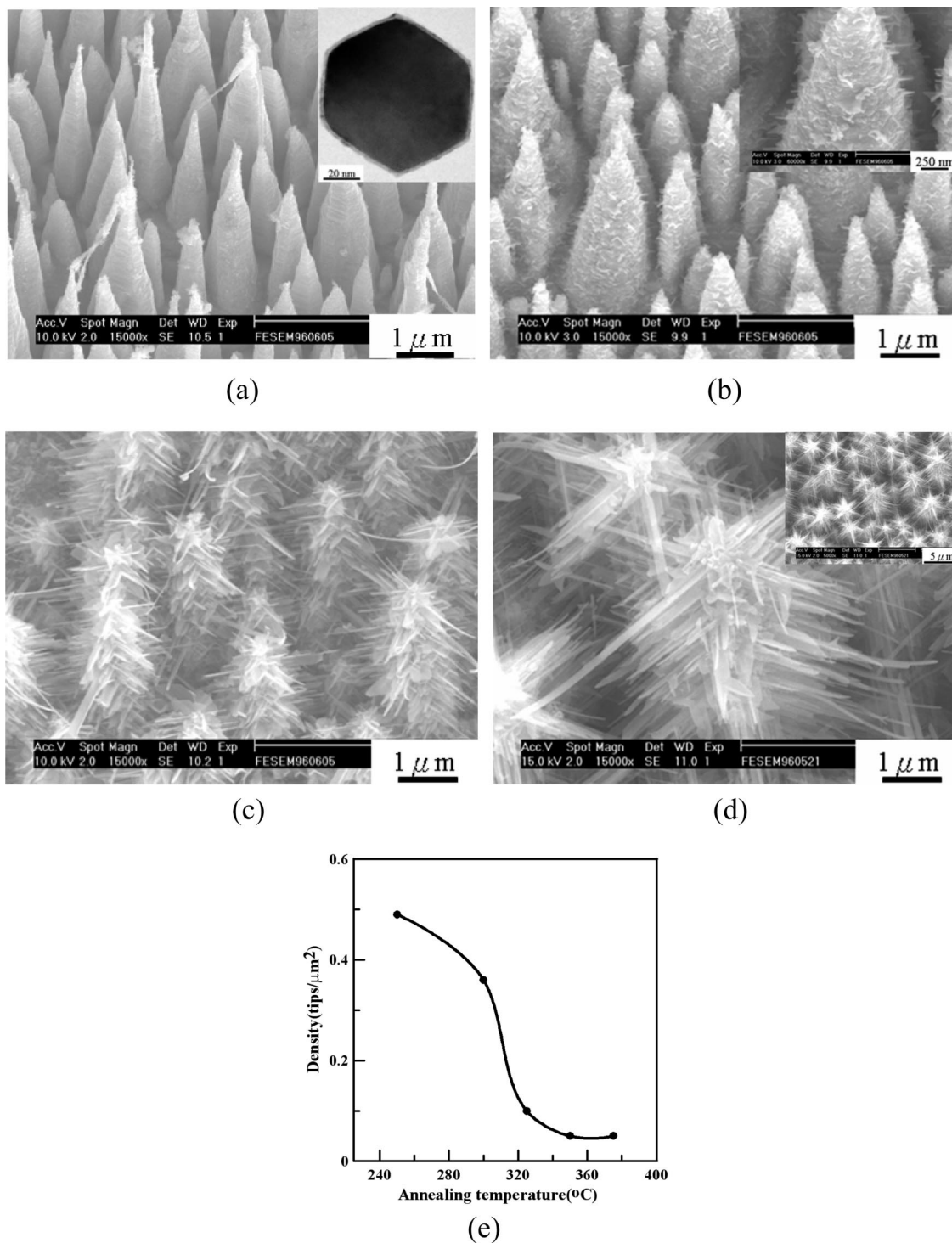


Figure 1. The SEM micrographs of arrays of Zn microtips before/after heat treatment. (a) original Zn microtip arrays and TEM microscopic image, (b–d) at different annealing temperatures (300, 325, 350 °C) for 12 h, and (e) illustrates the relationship between density and annealing temperature.

the low melting temperature of Zn. The Zn vapor mass transfer phenomenon cannot be observed directly, but can be determined if a detailed analysis of the Zn/ZnO interface is performed to realize the extensive vaporization of Zn during branch growth. There remain some underlying factors to be studied for fully understanding the role of Zn vapor transfer, and some further work is now under way. In brief, the specific growth direction for ZnO implies the preferred diffusion path for Zn atoms and their consequent reaction with oxygen vapor to grow ZnO branches (will be discussed in next paragraph).

The cross-section of the Zn/ZnO core–shelled hierarchical structure prepared by focused ion beam micromachining was examined by TEM as shown in Figure 4. From the TEM bright view it is clear to observe that the uniform shelled ZnO layer is formed between stem Zn and branched ZnO nanowhiskers, with a thickness of about 107 nm. The results of TEM image shown in Figure 4a clearly demonstrate that the nanowhiskers are longer on the edges, which could be the first sites of nucleation. However, the diffraction pattern inset of Figure 4b recorded from the interface including stem Zn and shelled ZnO

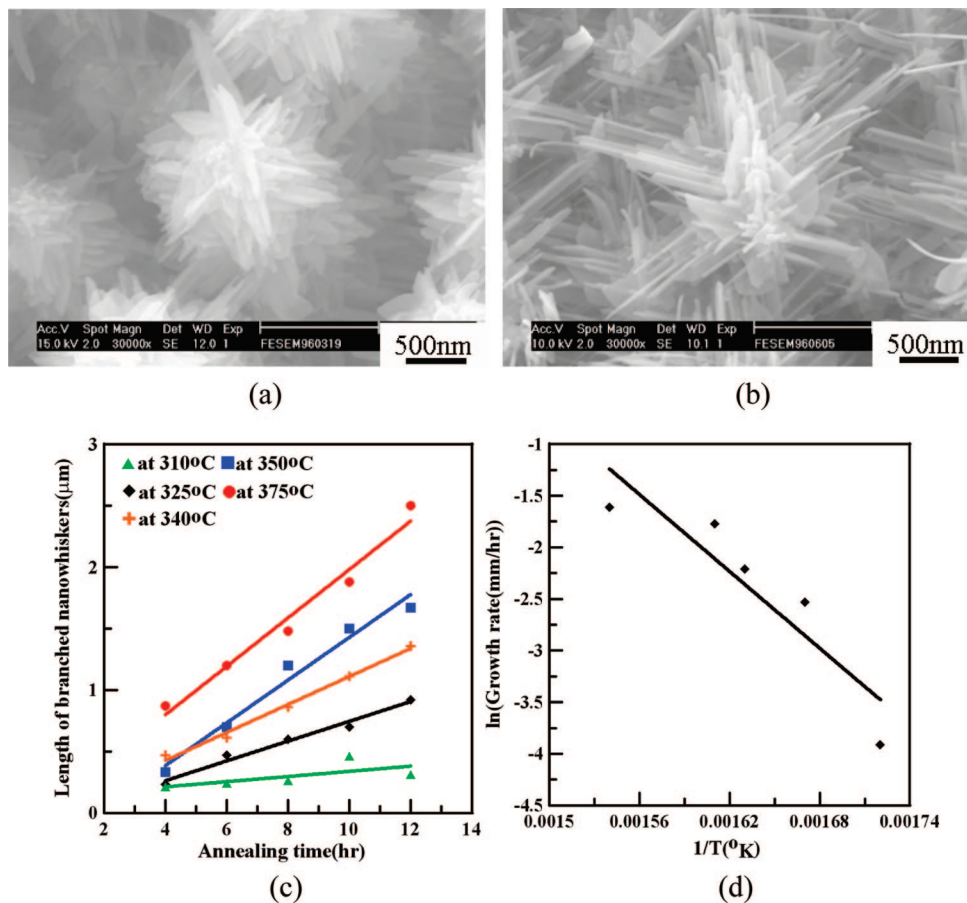


Figure 2. Hierarchical ZnO structures are obtained under different annealing times. (a) 6 h and (b) 10 h at 350 °C, and (c) a plot of the length of branches as a function of the reaction time at various temperatures (within the period 4–12 h); (d) Arrhenius plot for growth rate and the reciprocal of the treatment temperature.

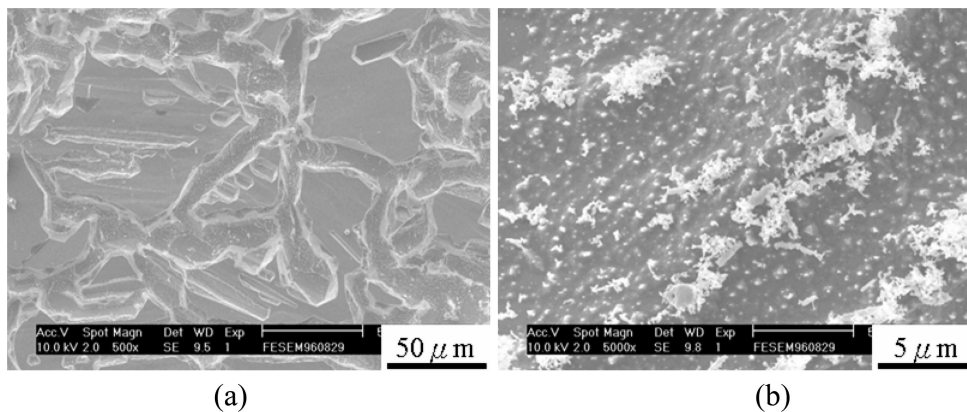


Figure 3. SEM images of Zn foil obtained under 10^{-6} torr vacuum atmosphere. (a) Polycrystalline foil and (b) single-crystalline Zn microtip arrays at 350 °C for 2 h.

indicates two sets of single-crystal diffraction spots, in which the zone axes are indexed to be $[1\bar{2}13]$ Zn and $[1\bar{2}13]$ ZnO with an epitaxial orientation. An enlargement of the atomic arrangement at the interface in Figure 4b is shown. At the boundaries of stem Zn and branched ZnO, the defects are induced by the lattice mismatch between Zn core and ZnO shell.¹⁷ The SAED patterns shown in inset of Figure 4c are obtained from branch sites, and indicate that ZnO nanowhiskers are with a single-crystalline structure and can be indexed to the hexagonal close packed (HCP) structure. An analysis of high-resolution TEM image shows a lattice spacing of 0.28 nm corresponding to the d spacing of the $\{1010\}$ crystal planes as

shown in Figure 4c. The distinct growth orientation for branched ZnO nanostructures along $[2\bar{1}10]$ is identified on isolated nanostructures taken from the sample (not shown here). In the present study, the mechanism for ZnO nanowhisker growth is a solid–gas process owing to the fact that the operating temperature is lower than the melting point of Zn.¹⁸ The source of Zn atoms for the branch growth are self-diffusion from the core Zn microtips to the surface. However, the specific growth feature of branches can be explained as follows: the ZnO nanowhiskers are closed by the $\pm(0001)$ planes on the top and bottom sides, where the alternate atomic layers in the (0001) planes may be particularly suitable for the transport of Zn atoms

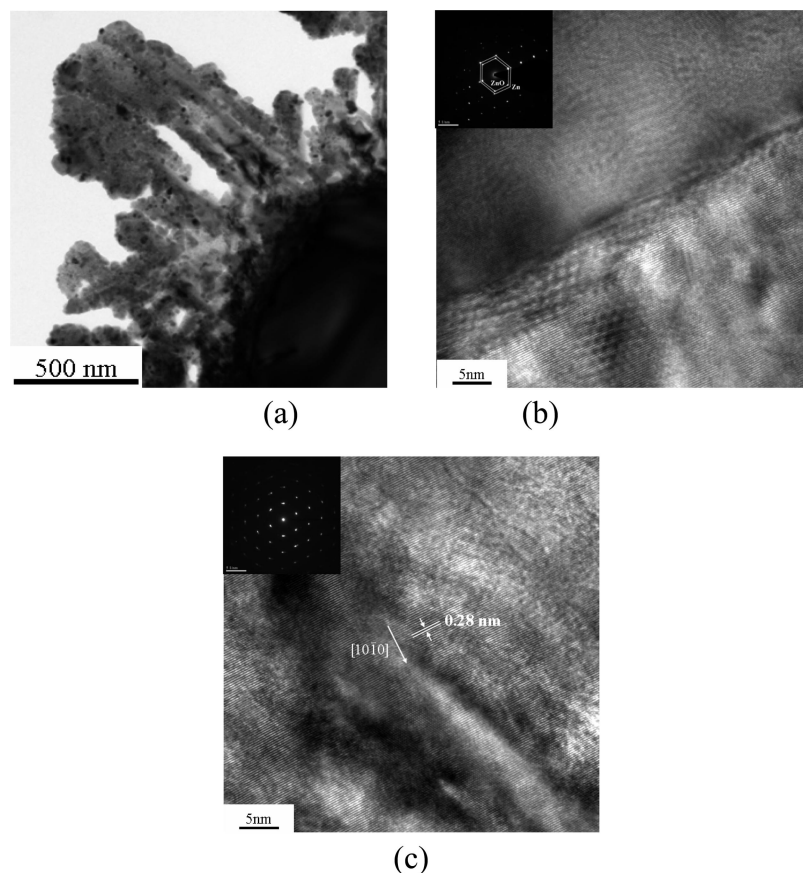


Figure 4. TEM results of hierarchical structure (a) bright-field image, (b) a high-resolution TEM image of stem Zn/ZnO shell, and (c) a high-resolution TEM image of branched ZnO nanowhiskers.

from the roots to the tips of the branched ZnO because each layer consists of a single type of atoms.⁸ In brief, the mechanism in the study differs from the conventional vapor-phase method because no evaporation phenomenon occurred in the experimental procedure. Besides, from the above diffraction patterns, the crystallography relationship among core Zn, shelled ZnO, and branched ZnO nanostructure is parallel to each other.

The conventional thermal evaporation method is widely adopted in the synthesis of metal oxide nanostructures.⁵ In comparison, the direct oxidation of metallic foil provides a simple, convenient, and fast method for synthesizing metal oxide nanostructures. In direct annealing of metallic foil, there are two major mechanisms proposed: (1) self-catalyst mechanism,¹⁹ and (2) relaxation of stress.¹⁶ But the operating temperature for self-catalyst is usually above the melting temperature of metallic foil, and the mechanism is not probable in the present study. A dense oxide film is formed on zinc microtips when the operating temperature is below the melting temperature of Zn foil (419.5 °C)²⁰ as shown in Figure 4a. During continuous oxidation processes, the stress will be generated and accumulated in oxide layer, and the two principal sources of stress are growth stresses and thermal stresses. The most important growth stresses are attributed to the volume difference between the oxide and the metal, epitaxial stresses, specimen geometry, etc.²¹ In the present study, the growth of a thin oxide layer on Zn microtips generally encounters with the issue of incompatibility of two crystalline lattices, and results in a mismatch at the Zn/ZnO interface. The different molar volume for Zn (9.1 cm³) and ZnO (14.2 cm³) induces an isotropic growth strain as given by the Pilling-Bedworth ratio (PBR) model.²² However, an important source of growth stresses arises due to the finite size of specimens and

the resultant curvature. The nature of stress developed will depend on the curvature and mechanism of scale growth. For the formation of oxide layer on convex/concave surfaces, the continued oxide formation at the interface can result in tensile/compressive stress development in the outer regions. In this study, the corners of the distinct Zn polyhedron are the energetically favorable sites owing to the curvature for concentrating stress.²³ The growth behavior of branched nanostructures on the microtip arrays corresponds to the results of TEM analysis. In general, the symmetry of the hierarchical structure is decided by the shape of core. A spherical shell composed of radiating nanobelts is obtained by direct annealing of a Zn microparticle⁷ and multifold (2-, 4-, 6-fold) symmetrically hierarchical structures also have been successfully grown of the case of indium oxide.²⁴ Therefore, the formation of distinct 6-fold hierarchical structure can be further confirmed due to the symmetric polyhedron. The formation mechanism for 6-fold hierarchical structures can be simply described as a combination of the symmetric microtip arrays and the volume expansion caused by the formation of oxide layer followed by solid–gas reaction.

Figure 5a shows the result of field emission characteristics of single-crystalline Zn microtips before and after annealing at different temperatures (250, 325, 350, and 375 °C) for 12 h, respectively. The turn-on electric fields for Zn microtip arrays and hierarchical structures obtained at different annealing temperatures are 33.9, 20.0, 33.3, 32.6, and 8.5 V/μm (obtained respectively at the separation of 30, 30, 30, 30, and 60 μm), respectively. So far, it is well-known that the field-emission performance is related to the morphology, density, crystal size, and the intrinsic properties of materials.²⁵ The field emission

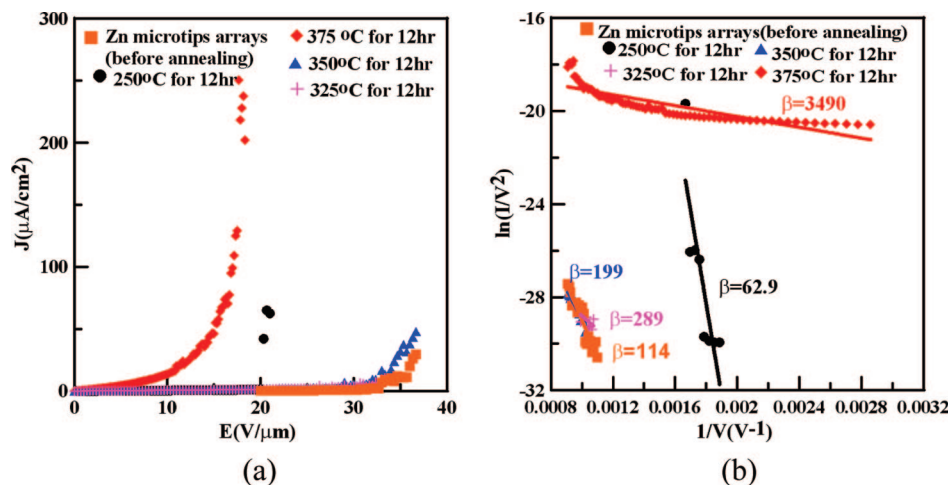


Figure 5. (a) J - E curves for the field emission behavior of the core-shell structures, and (b) the FN plot.

properties can be discussed in terms of their structures, as can be divided into two kinds by apparent morphology; one is the thin oxide layer on the surface obtained with 250–300 °C annealing, and the other is 6-fold hierarchical structure obtained with 325–375 °C annealing. In the initial reaction, an enhanced emission result can be obtained by Zn microtip arrays with 250 °C annealing, and the thin oxide layer is on Zn to form the Zn/ZnO core-shelled structure. The improvement of field emission can be explained by the presence of wide bandgap materials formed on the surface with an optimum thickness.²⁶ For the 6-fold hierarchical structure arrays, the field emission performances of turn on voltage are enhanced from 33.3 to 8.5 V/ μm . By increasing the length of branched nanostructures, the turn-on electric fields for emission features are further improved. For 1D nanostructures, an easier electron penetration for field emission resulted from the higher aspect ratio.²⁷ The aspect ratio of branched ZnO increased from 26 to 71 results in the improvement of emission features as annealing temperature is increased from 325 to 375 °C. A linear relationship of the Fowler-Nordheim (FN) curves within the measurement ranges, as shown in Figure 5b, is observed and the field enhancement factor β can be calculated by assuming a work function of 4.3 and 5.3 eV for Zn and ZnO, respectively. The enhancement factor β is estimated to be about 114, 62.9, 289, 199, and 3490 for the single-crystalline Zn microtip arrays, Zn/ZnO shelled (250 °C), and hierarchical structure with different annealing temperature (325, 350, and 375 °C), respectively. The field emission property of 3D hierarchical structure is related to the density of hierarchical structures arrays and the length of branches. The emission property of thermal oxidized metallic foil is also illustrated for the case of brass foil after thermal oxidation,^{9,28} and electrochemical route.²⁹ In comparison, the emission characteristics of 6-fold hierarchical structure are not significantly improved. Herein, the highest enhancement factor of 3490 is superior to the hierarchical structures obtained by direct annealing brass foil,⁹ and illustrates the possible applications for the novel 3D hierarchical structures. In brief, the emission characteristics are improved to 20 V/ μm by forming a shell oxide layer on the Zn microtip arrays, and then, further enhanced to 8.5 V/ μm by branch growth on Zn microtips.

Conclusion

In summary, this paper reports the metal-based microtip arrays that have a distinct hierarchical morphology synthesized by a

direct annealing treatment. The 6-fold symmetric hierarchical structure composed of stem Zn, shelled ZnO layer, and branched ZnO nanostructures is guided by the symmetric polyhedron microtip arrays. The influence of annealing temperature and time on the growth kinetics for the branched nanostructures is illustrated, and the effect of annealing temperature is identified. With changing annealing temperature, the different morphology and density of the hierarchical arrays are obtained. The growth rate of the branches is obtained, and the activation energy is identified by kinetics analysis. Besides, the source of possible anisotropic stresses for branched nanostructure growth is also discussed. By TEM observation, the epitaxial orientation among core Zn, shelled ZnO layer, and branched ZnO nanostructure is identified. The density and the aspect ratio of branched nanostructures are the crucial elements for emission property. To date, the regularity and multidimensional patterned arrays are not obtained yet under a direct oxidation process. However, the 3D hierarchical arrays can be obtained by the well anisotropically orientated Zn polyhedron under direct annealing processes, and provide an alternative methodology for the preparation and application of other nanostructures with symmetric arrays.

Acknowledgment. The financial support of this study from the National Science Council through contracts NSC96-2221-E-006-007, NSC96-2221-E-006-119-MY3, and NSC 95-2221-E-239-025 is greatly appreciated. The technical assistance from the Center for NanoScience & NanoTechnology NSYSU and NSC Core Facilities Laboratory in Kaohsiung-Pingtung Area is also appreciated.

References

- (1) Kong, X. Y.; Wang, Z. L. *Nano Lett.* **2003**, *3*, 1625.
- (2) Vayssieres, L. *Adv. Mater.* **2003**, *15*, 464.
- (3) Wang, Y. C.; Leu, I. C.; Hon, M. H. *Electrochem. Solid State Lett.* **2002**, *5*, C53.
- (4) Li, W. J.; Shi, E. W.; Zhong, W. Z.; Yin, Z. W. *J. Cryst. Growth* **1999**, *203*, 186.
- (5) Dick, K. A.; Deppert, K.; Larsson, M. W.; Martensson, T.; Seifert, W.; Wallengren, L. R.; Samuelson, L. *Nat. Mater.* **2004**, *3*, 380.
- (6) Zhang, T.; Dong, W.; Brewer, M. K.; Konar, S.; Njabon, R. N.; Tian, Z. R. *J. Am. Chem. Soc.* **2006**, *128*, 10960.
- (7) Jiang, X. C.; Herricks, T.; Xia, Y. N. *Nano Lett.* **2002**, *2*, 1333.
- (8) Wen, X. G.; Fang, Y. P.; Pang, Q.; Yang, C. L.; Wang, J. N.; Ge, W. K.; Wong, K. S.; Yang, S. H. *J. Phys. Chem. B* **2005**, *109*, 15303.
- (9) Zhu, Y. W.; Sow, C. H.; Yu, T.; Zhao, Q.; Li, P. H.; Shen, Z. X.; Yu, D. P.; Thong, J. T. L. *Adv. Funct. Mater.* **2006**, *16*, 2415.

- (10) Fan, H. J.; Scholz, R.; Kolb, F. M.; Zacharias, M. *Appl. Phys. Lett.* **2004**, 85, 4142.
- (11) Kuan, C. Y.; Chou, J. M.; Leu, I. C.; Hon, M. H. *Electrochem. Commun.* **2007**, 9, 2093.
- (12) Nakamura, R.; Lee, J. G.; Tokozakura, D.; Mori, H.; Nakajima, H. *Mater. Lett.* **2007**, 61, 1060.
- (13) Zhang, T.; Dong, W.; Njabon, R. N.; Varadan, V. K.; Tian, Z. R. *J. Phys. Chem. C* **2007**, 111, 13691.
- (14) Moore, W. J.; Lee, J. K. *Trans. Faraday Soc.* **1950**, 47, 501.
- (15) Kubaschewski, O.; Hopkins, B. E. *Oxidation of Metals and Alloys*; Butterworths: London, 1967.
- (16) Kumar, A.; Srivastava, A. K.; Tiwari, P.; Nandedkar, R. V. *J. Phys.: Condens. Matter* **2004**, 16, 8531.
- (17) Kong, X. Y.; Ding, Y.; Wang, Z. L. *J. Phys. Chem. B* **2004**, 108, 570.
- (18) Liu, Y. L.; Pan, C. X.; Dai, Y.; Chen, W. *Mater. Lett.* **2008**, 62, 2783.
- (19) Dang, H. Y.; Wang, J.; Fan, S. S. *Nanotechnology* **2003**, 14, 738.
- (20) Ren, S.; Bai, Y. F.; Chen, J.; Deng, S. Z.; Xu, N. S.; Wu, Q. B.; Yang, S. *Mater. Lett.* **2007**, 61, 666.
- (21) Birks, N.; Meier, G. H. *Introduction to High Temperature Oxidation of Metals*; Edward Arnold: London, 1983.
- (22) Panicaud, B.; Grosseau-Poussard, J. L.; Dinhut, J. F. *Appl. Surf. Sci.* **2006**, 252, 5700.
- (23) Carim, A. H.; Sinclair, R. *J. Electrochem. Soc.* **1987**, 134, 741.
- (24) Lao, J. Y.; Wen, J. G.; Ren, Z. F. *Nano Lett.* **2002**, 2, 1287.
- (25) Suh, J. S.; Jeong, K. S.; Lee, J. S.; Han, I. *Appl. Phys. Lett.* **2002**, 80, 2392.
- (26) Yi, W. K.; Jeong, T. W.; Yu, S. G.; Heo, J. N.; Lee, C. S.; Lee, J. H.; Kim, W. S.; Yoo, J. B.; Kim, J. M. *Adv. Mater.* **2002**, 14, 1464.
- (27) Jo, S. H.; Tu, Y.; Huang, Z. P.; Carnahan, D. L.; Wang, D. Z.; Ren, Z. F. *Appl. Phys. Lett.* **2003**, 82, 3520.
- (28) Huo, K. F.; Hu, Y. M.; Fu, J. J.; Wang, X. B.; Chu, P. K.; Hu, Z.; Chen, Y. *J. Phys. Chem. C* **2007**, 111, 5876.
- (29) Cao, B. Q.; Teng, X. M.; Heo, S. H.; Li, Y.; Cho, S. O.; Li, G. H.; Cai, W. P. *J. Phys. Chem. C* **2007**, 111, 2470.

CG800373U